PNAS
www.pnas.org

Supplementary Information for

A PRC2-KDM5B axis sustains tumorigenicity of acute myeloid leukemia

Zhihong Ren[a,b,1,#], Arum Kim[a,b,1], Yu-Ting Huang[c,2], Wen-Chieh Pi[c,2], Weida Gong[a], Xufen Yu[d], Jun Qi[e], Jian Jin[d], Ling Cai[a,b,f], Robert G. Roeder[g,3], Wei-Yi Chen[c,h,3], Gang Greg Wang[a,b,i,3]

[3]Correspondence authors:
Robert G. Roeder
Contact: roeder@rockefeller.edu

Wei-Yi Chen
Contact: chenwy@nycu.edu.tw

Gang Greg Wang
Contact: greg_wang@med.unc.edu

This PDF file includes:

Supplementary Materials and Methods

Plasmid construction

The cDNA of murine *Kdm5b* (NM_152895.2) was cloned into the MSCV-puro retroviral vector, with Flag or GFP tag added in-frame to its N-terminus. *Kdm5b* mutants were created by site-directed mutagenesis as described before [1, 2]. For knockdown (KD) of murine *Kdm5b* (Sigma, cat# TRCN0000113491; with the hairpin sequence as GCCTACATCATGTGAAAGAAT) or human *EZH2* gene (Sigma, cat# TRCN0000018365; with the hairpin sequence as TATGATGGTTAACGGTGATCA), the pLKO.1-puro based lentiviral shRNA was purchased from Sigma and used according to vendor-recommended manuals.

Tissue culture and cell lines

Murine AML cell lines carrying NUP98-NSD1 (Flag-tagged) or MLL-r were previously described [3-5]. In brief, lineage-negative hematopoietic stem and progenitor cells (HSPCs) isolated from BALB/C mice were stably transduced with the oncogene, followed by transplantation to syngeneic mice. The murine AML cells were derived from bone marrow of leukemic mice and maintained in the OptiMEM base medium supplemented with 15% of FBS, 50uM of beta-mercaptoethanol, 1% of penicillin and streptomycin, and murine stem cell factor (mSCF; added with 10% of supernatant from a mSCF-secreting Chinese hamster ovary cell line). Human cell lines including MV4;11 (American Tissue Culture Collection [ATCC], CRL-9591), MOLM13 (Deutsche Sammlung von Mikroorganismen und Zellkulturen [DSMZ], ACC-554) and HEK293T (ATCC CRL-3216) were maintained using vendor-recommended culture conditions. To establish the stable cell lines, retrovirus or lentivirus was prepared with the packaging system in HEK293T cells, followed by cell infection and drug selection as we described before [1, 2, 6]. Authentication of cell line identities was ensured by the Tissue Culture Facility (TCF) affiliated to UNC Lineberger Comprehensive Cancer Center with the genetic signature profiling analysis. Every 1-2 months, a routine examination of cells for potential mycoplasma contamination was performed using the commercially available detection kits (Lonza).

Antibodies and western blot

The immunoblotting was conducted with the total cell lysate as we reported before [1, 2, 6]. Antibodies used in this study are listed in Dataset S7.

Chemicals

UNC1999 [5, 7, 8] and JQEZ5 [9, 10] were synthesized and used as previously reported.

Phenotypic assays of hematological cells, such as colony-forming unit (CFU), Wright-Giemsa staining and proliferation assay

Assays for CFU using a methylcellulose-based culture system (STEMCELL Technologies, M3434), Wright-Giemsa staining, and counting-based cell proliferation were carried out as we described before [1, 5, 11].

Assays of cell cycle progression and apoptosis

To measure cell cycle progression, cells were collected by centrifugation, washed with ice-cold PBS, and fixed in pre-chilled 80% methanol. Cell staining was then conducted in PBS plus 20 μg/mL of propidium iodide (Sigma), 0.1% of Triton-X100 and 200 μg/mL of RNase A (Roche). DNA contents of cells were measured with a CyAnADP flow cytometer (Beckman-Coulter) and then analyzed by ModFit Software to define the status of cell cycle progression (VeritySoftware). Apoptosis was measured with the Annexin V-FITC Apoptosis Detection Kit (BD, 556570), followed by analysis with the CyAnADP flow cytometer and then analysis with the FlowJo Software (BD).

In vivo leukemogenic studies

All animal experiments were performed according to the protocol approved by Institutional Animal Care and Use Committee (IACUC), University of North Carolina (UNC). Murine AML was established by injection of 0.5 million of the already established murine AML cell lines (stably labeled with a luciferase-IRES-GFP reporter) via tail vein into syngeneic BALB/C mice (Jackson Laboratory) as described [1, 5, 11]. All mice were housed according to the guidelines of UNC

Animal Studies Core. Animal care, monitoring of leukemogenesis such as weekly chemiluminescence imaging of live animals and treatment with compounds were performed using the same protocols described before [1, 5, 11].

RNA sequencing and data analysis

RNA-seq was performed as previously described [2, 6, 12]. In brief, total RNA was extracted by using RNeasy Plus Mini Kit (Qiagen) and RNA libraries prepared by using the NEBNext Ultra II RNA Library Prep Kit (NEB). Multiplexed RNA-seq libraries were subjected to deep sequencing using the Illumina Hi-Seq 2000/2500 platform according to the manufacturer's instructions (UNC-Chapel Hill High-Throughput Sequencing Facility). Analysis of RNA-seq data and Gene Set Enrichment Analysis (GSEA) with the RNA-seq profiles were conducted as before [1, 2, 6]. In brief, the fastq files were aligned to the mm10 mouse genome (GRCm38.p4) using STAR v2.4.2 [13] with the following parameters: --outSAMtype BAM Unsorted --quantMode TranscriptomeSAM. Transcript abundance for each sample was estimated with salmon v0.1.19 [14] to quantify the transcriptome defined by Ensembl annotation. Gene level counts were summed across isoforms and genes with low counts (maximum expression < 10) were filtered for the downstream analyses. We tested genes for differential expression in DESeq2 v1.38.2 [15].

Chromatin immunoprecipitation (ChIP) followed by sequencing (ChIP-Seq) and data analysis

ChIP-seq was performed according to our previously described protocol [1, 2, 6], with antibodies used in this study are listed in Dataset S7. The produced libraries were subjected to deep sequencing with the Illumina High-Seq 2000/2500 platform according to the manufacturer's instructions (available at the UNC-Chapel Hill High-Throughput Sequencing Facility). ChIP-seq data analysis and profile visualization with Integrative Genomics Viewer (IGV; Broad Institute) were conducted as described before [1, 2, 12, 16].

Analysis of publicly available patient datasets.

The publicly available gene-expression datasets used in the study included the TCGA AML cohort (https://portal.gdc.cancer.gov) and NCBI Gene Expression Omnibus (GEO) accession numbers GSE68833 (TCGA), GSE10358 and GSE14468. To correlate patient clinical outcome with the matched transcriptome profiling, we processed the downloaded datasets with Partek Genomics Suite (Version 6.6), followed by assessment of correlation between gene expression and patient survival as before [7] by using the Kaplan-Meier and Cox survival analysis tools of the Suite according to users' manuals.

RT followed by real-time quantitative PCR (RT-qPCR)

Total RNAs were converted to cDNA with the iScript cDNA Synthesis Kit (Bio-Rad, 1708890). Quantitative PCR was performed in triplicate using the iTaq Universal SYBR Green Supermix (Bio-Rad, 1725124). RT-qPCR was conducted with the QuantStudio 6 Flex real-time PCR system (Applied Biosystems) as described before [7, 17]. Primers used for RT-qPCR are listed in Dataset S7.

Cleavage Under Targets & Release Using Nuclease (CUT&RUN)

CUT&RUN was performed according to manufacturer's instruction (EpiCypher CUTANA™ pAG-MNase for ChIC/CUT&RUN, Cat# 15-1116) as we described [2, 18]. Antibodies used in this study are listed in Dataset S7. In brief, 0.5 million of cells were rinsed with the wash buffer (20 mM HEPES, pH 7.5, 150 mM NaCl, 0.5 mM Spermidine, and 1× Complete Protease Inhibitor Cocktail) and incubated with the activated Concanavalin A (ConA) beads (Bangs Laboratories BP531) at room temperature for 10 minutes, followed by addition of antibody (1:50 dilution) and incubation at 4 degree overnight. After permeabilization with digitonin buffer (the above wash buffer plus 0.01% digitonin), samples were subject to the digestion with pAG-MNase, and solubilized chromatin released. Then, DNA purification was performed with the PCR cleanup kit (NEB, Monarch PCR & DNA Cleanup Kit, T1030), and DNA libraries prepared by using the NEB Ultra II DNA Library Prep Kit (NEB #E7103). Sequencing was carried out using the Illumina NextSeq 500 Sequencing System and CUT&RUN data analysis conducted as we described before [1, 18].

Statistics and reproducibility

All data from representative experiments (such as western blotting, flow and imaging) were repeated two to three times independently with similar results. Data shown in bar plot are presented as mean ± SD of three independent experiments unless otherwise noted. Statistical analysis was performed with two-sided Student's t test for comparing two sets of data with assumed normal distribution. We used a two-sided log-rank test for Kaplan-Meier survival curves to determine statistical significance. A *P* value of less than 0.05 was considered significant. Statistical significance levels are denoted as follows: **P* <0.05; ***P* <0.01; ****P* <0.001; *****P* <0.0001. No statistical methods were used to predetermine sample size.

Data availability

RNA-seq, ChIP-seq and CUT&RUN datasets related to this work have been deposited in the NCBI GEO under accession number GSE179826.

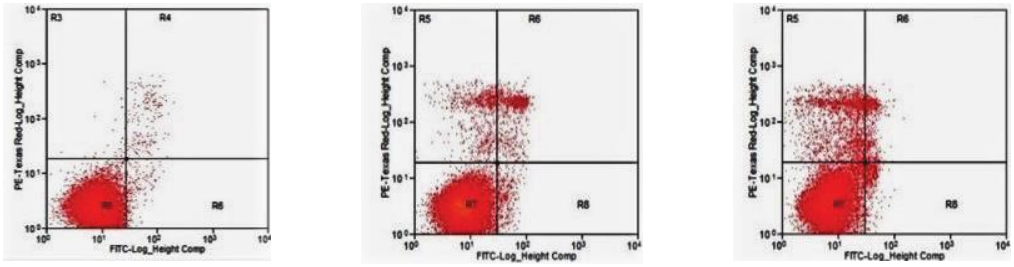

DMSO

UNC1999 1uM
3 days

UNC1999 3uM
3 days

Fig. S1. The representative flow cytometric diagram for assessing apoptotic phenotypes in NUP98-NSD1+ AML cells after treatment with UNC1999.

A

Sample	Replicate #	Total # of reads	# of uniquely mapped reads
DMSO	1	17,547,162	13,729,853
	2	15,474,280	12,134,636
	3	17,412,284	13,621,136
JQEZ5	1	21,220,639	16,814,569
	2	18,507,576	14,744,874
	3	17,437,536	13,800,911
UNC1999	1	19,438,321	15,525,318
	2	17,189,265	13,857,790
	3	14,240,679	11,509,537

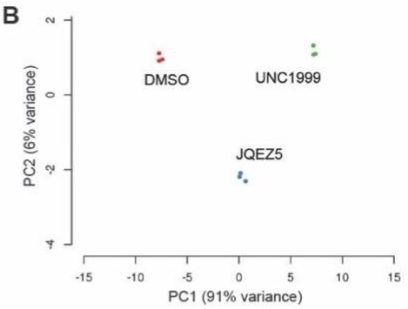

C

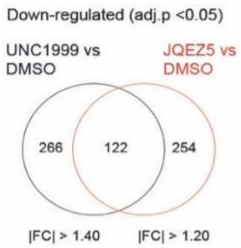

D

	DMSO vs UNC1999			DMSO vs JQ-EZ5		
MSigDB Gene Set	NES	NOM p	FDR q	NES	NOM p	FDR q
Polycomb-related						
PRC2_EED2_UP.V1_DN	1.340	0.018	0.088	1.450	0.000	0.019
PRC2_EZH2_UP.V1_UP	-1.380	0.000	0.039	-1.830	0.000	0.000
Cell cycle related						
HALLMARK_E2F_TARGETS	1.780	0.000	0.002	2.850	0.000	0.000
HALLMARK_G2M_CHECKPOINT	1.710	0.000	0.002	2.480	0.000	0.000
Cell death related						
HALLMARK_APOPTOSIS	-1.520	0.003	0.026	-1.550	0.004	0.010
Hematopoietic stem cell related						
JAATINEN_HEMATOPOIETIC_STEM_CELL_DN	-1.620	0.000	0.093	-2.010	0.000	0.000
Leukemia related						
GO_MYELOID_LEUKOCYTE_DIFFERENTIATION	-1.300	0.045	0.267	-1.620	0.003	0.021

E

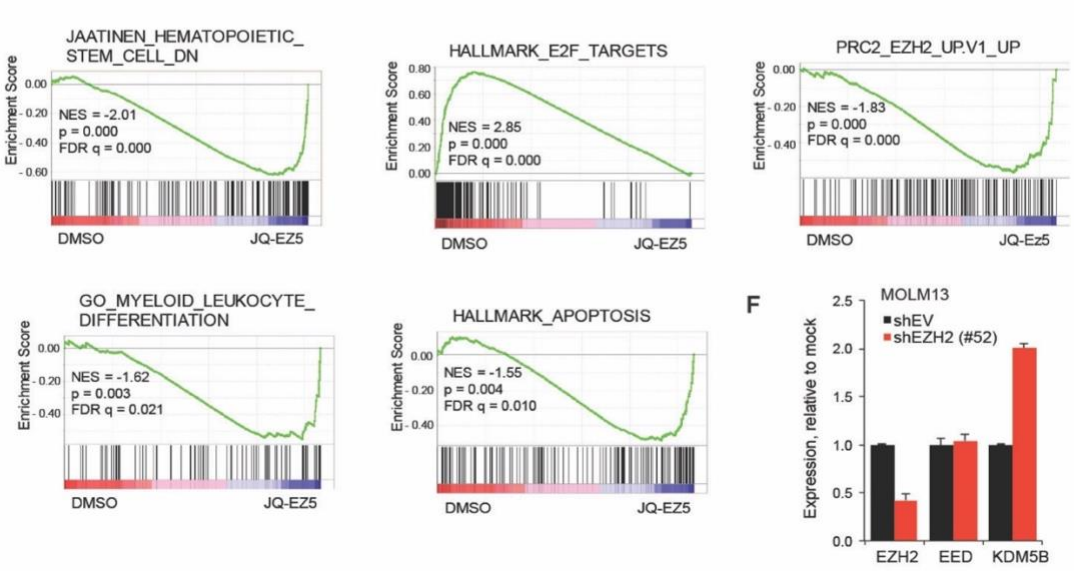

F

Fig. S2. Kdm5b, a tumor suppressor of AML, is a direct target of PRC2 and H3K27me3 in AML. (A-B) Summary of sequencing read counts (A) and Principal Component Analysis (PCA) using RNA-seq data of NUP98-NSD1+ AML cells treated with DMSO, 3 μM of UNC1999 or JQEZ5 for 3 days (n =3 replicated experiments). (C) Venn diagram showing the overlap between differentially expressed genes (DEGs) identified by RNA-seq to be down-regulated after a 3-day treatment with 3 μM of either EZH2 inhibitor, UNC1999 (left) or JQEZ (right), versus DMSO in NUP98-NSD1+ murine AML cells. (D) Summary of Gene Set Enrichment Analysis (GSEA) using the Molecular Signatures Database (MSIgDB), which reveals the indicated gene sets to be correlated with treatment of UNC1999 (left) or JQEZ5 (right), relative to mock. (E) GSEA revealing that JQEZ5 treatment is correlated positively to gene sets repressed by PRC2 or related to leukocyte differentiation or apoptosis in NUP98-NSD1+ murine AML cells. (F) RT-qPCR of EZH2, EED and Kdm5b following EZH2 depletion (shEZH2 #52) in the MOLM-13 human AML cells carrying MLL-r+.

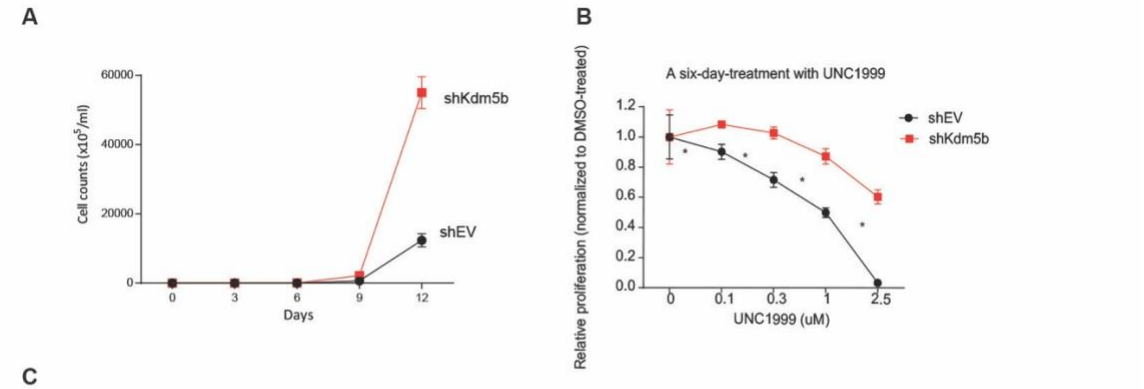

C

	EV vs Kdm5b KD		
MSigDB Gene Set	**NES**	**NOM p**	**FDR q**
Hematopoietic stem cell related			
GO_HEMATOPOIETIC_STEM_CELL_DIFFERENTIATION	1.83	0.000	0.005
RAMALHO_STEMNESS_DN	1.75	0.002	0.011
GO_REGULATION_OF_STEM_CELL_DIFFERENTIATION	1.53	0.010	0.051
Histone methylation related			
MIKKELSEN_ES_ICP_WITH_H3K4ME3	-1.82	0.000	0.008

D

	Kdm5b_exp. vs EV		
MSigDB Gene Set	**NES**	**NOM p**	**FDR q**
Hematopoietic stem cell related			
RAMALHO_STEMNESS_DN	2.27	0.000	0.000
JAATINEN_HEMATOPOIETIC_STEM_CELL_DN	2.13	0.000	0.000
GAL_LEUKEMIC_STEM_CELL_DN	1.55	0.001	0.045
Histone methylation related			
MIKKELSEN_NPC_HCP_WITH_H3K4ME3_AND_H3K27ME3	-1.62	0.013	0.065
MEISSNER_NPC_HCP_WITH_H3K4ME2_AND_H3K27ME3	-1.54	0.010	0.061
MEISSNER_NPC_HCP_WITH_H3K4ME3_AND_H3K27ME3	-1.52	0.017	0.045
Cell cycle related			
HALLMARK_E2F_TARGETS	-2.69	0.000	0.000
HALLMARK_G2M_CHECKPOINT	-2.11	0.000	0.000
GO_CELL_CYCLE_DNA_REPLICATION	-1.76	0.000	0.015
GO_CELL_CYCLE_G2_M_PHASE_TRANSITION	-1.41	0.000	0.052
Cell death related			
HALLMARK_APOPTOSIS	1.33	0.056	0.135

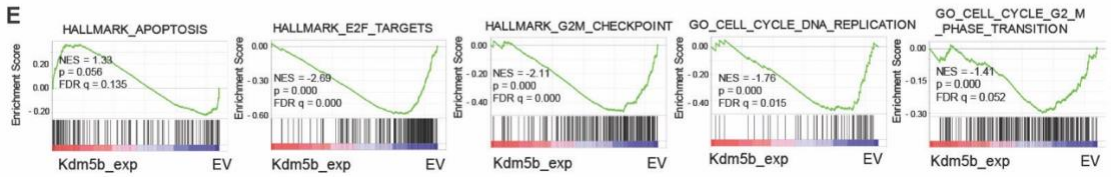

Fig. S3. Depletion of Kdm5b not only renders AML cells unresponsive to PRC2 inhibition but also promotes aggressiveness of AML. (A) Proliferation of NUP98-NSD1-transformed murine AML cells after Kdm5b depletion (shKdm5b), relative to control (shEV; n=3 independent experiments; presented as the mean ± SD). (B) Relative proliferation of the indicated control (shEV) or Kdm5b-depleted (shKdm5b) NUP98-NSD1+ AML cells after treatment with a range of concentrations of UNC1999 for 6 days. Y-axis represents the relative cell numbers normalized to DMSO treatment (n=3 independent experiments; presented as the mean ± SD). *, p<0.05. (C-E) GSEA of RNA-seq profiles revealed that, relative to control (EV), Kdm5b depletion (KD in panel C) is negatively correlated to differentiation-related gene sets while ectopic expression of WT Kdm5b (Kdm5b_exp in panel D) is positively correlated to differentiation- and apoptosis-related gene sets, with the representative GSEA results shown in E.

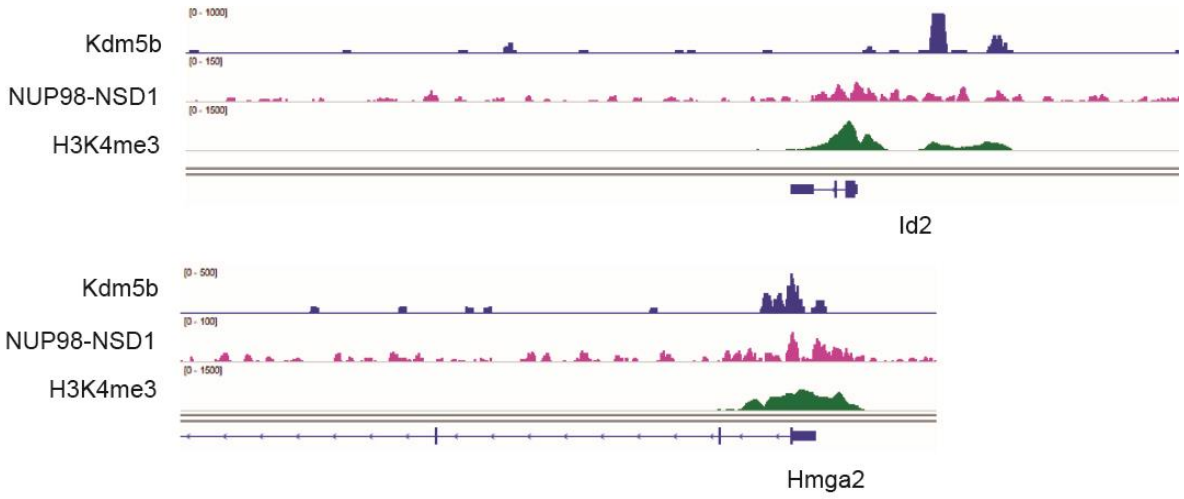

Fig. S4. Kdm5b and NUP98-NSD1 directly bind to stemness and AML-causing genes.
IGV screen shots showing ChIP-seq profiles (after input depth normalization) of Kdm5b, NUP98-NSD1 (Flag-tagged) and H3K4me3 at the indicated cancer-related genes, Id2 and Hmga2, in NUP98-NSD1+ murine AML cells.

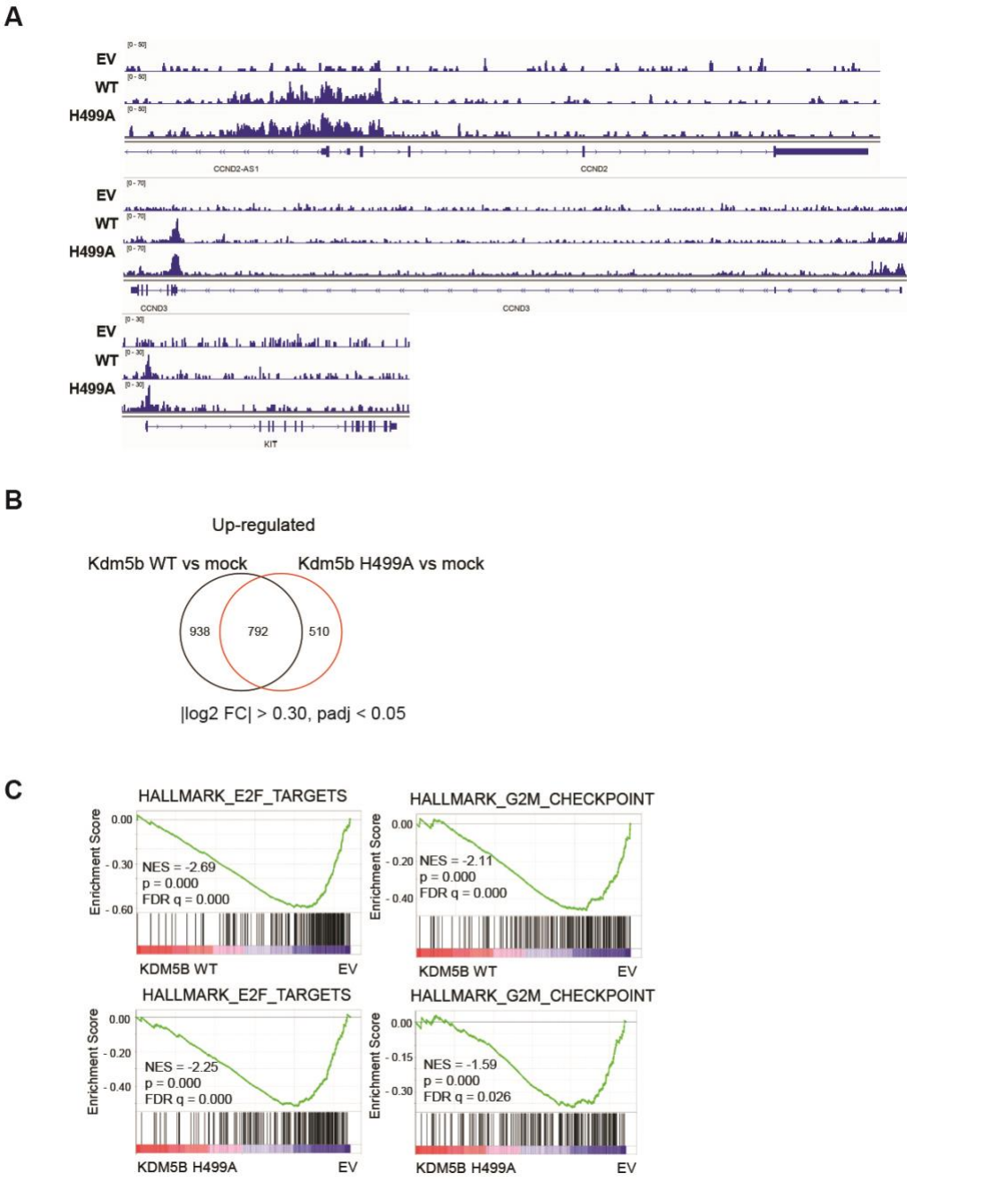

Fig. S5. The demethylase function of Kdm5b is dispensable for its tumor suppressive role in AML. (A) IGV screen shots showing GFP-Kdm5b CUT&RUN profiles at the indicated genes in HEK293 cells with the stable expression of EV (as anti-GFP CUT&RUN control) or GFP-tagged Kdm5b, either WT or H499A-mutated. (B) Venn diagram showing the significant overlap between DEGs found by RNA-seq to be up-regulated post-transduction of WT (left) or H499A-mutated (right) Kdm5b in MLL-AF9+ murine AML cells, relative to EV-transduced mock controls. (C) GSEA of RNA-seq data revealing that, relative to mock controls, ectopic expression of WT (top) or H499A-mutated (bottom) Kdm5b is negatively correlated with cell cycle progression-related gene sets Kdm5b in MLL-AF9+ murine AML cells.

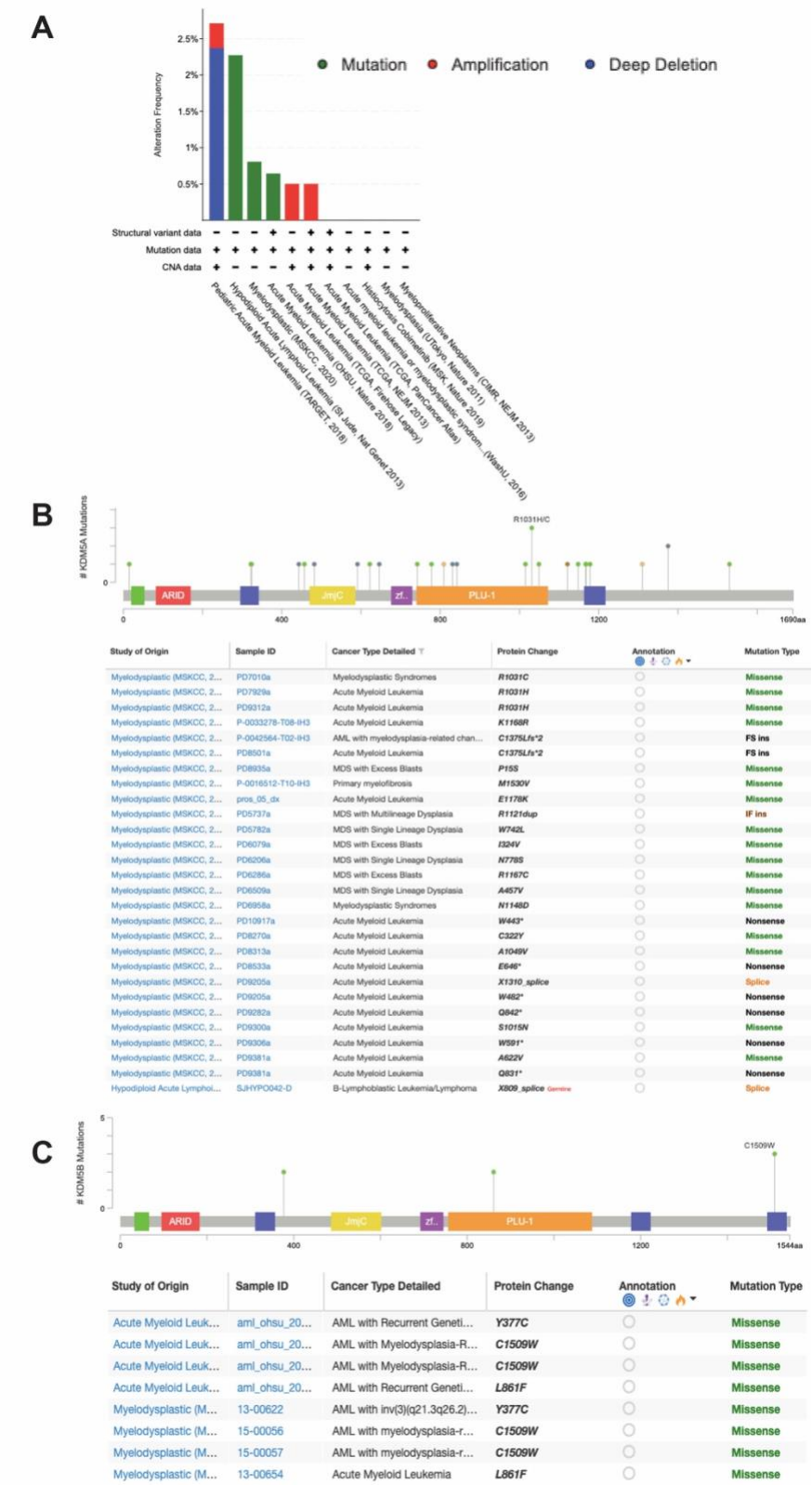

Study of Origin	Sample ID	Cancer Type Detailed	Protein Change	Annotation	Mutation Type
Myelodysplastic (MSKCC, 2...	PD7010a	Myelodysplastic Syndromes	R1031C		Missense
Myelodysplastic (MSKCC, 2...	PD7929a	Acute Myeloid Leukemia	R1031H		Missense
Myelodysplastic (MSKCC, 2...	PD9312a	Acute Myeloid Leukemia	R1031H		Missense
Myelodysplastic (MSKCC, 2...	P-0033278-T08-IH3	Acute Myeloid Leukemia	K1168R		Missense
Myelodysplastic (MSKCC, 2...	P-0042564-T02-IH3	AML with myelodysplasia-related chan...	C1375Lfs*2		FS ins
Myelodysplastic (MSKCC, 2...	PD8501a	Acute Myeloid Leukemia	C1375Lfs*2		FS ins
Myelodysplastic (MSKCC, 2...	PD8935a	MDS with Excess Blasts	P15S		Missense
Myelodysplastic (MSKCC, 2...	P-0016512-T10-IH3	Primary myelofibrosis	M1530V		Missense
Myelodysplastic (MSKCC, 2...	pros_05_dx	Acute Myeloid Leukemia	E1178K		Missense
Myelodysplastic (MSKCC, 2...	PD5737a	MDS with Multilineage Dysplasia	R1121dup		IF ins
Myelodysplastic (MSKCC, 2...	PD5782a	MDS with Single Lineage Dysplasia	W742L		Missense
Myelodysplastic (MSKCC, 2...	PD6079a	MDS with Excess Blasts	I324V		Missense
Myelodysplastic (MSKCC, 2...	PD6206a	MDS with Single Lineage Dysplasia	N778S		Missense
Myelodysplastic (MSKCC, 2...	PD6286a	MDS with Excess Blasts	R1167C		Missense
Myelodysplastic (MSKCC, 2...	PD6509a	MDS with Single Lineage Dysplasia	A457V		Missense
Myelodysplastic (MSKCC, 2...	PD6958a	Myelodysplastic Syndromes	N1148D		Missense
Myelodysplastic (MSKCC, 2...	PD10917a	Acute Myeloid Leukemia	W443*		Nonsense
Myelodysplastic (MSKCC, 2...	PD8270a	Acute Myeloid Leukemia	C322Y		Missense
Myelodysplastic (MSKCC, 2...	PD8313a	Acute Myeloid Leukemia	A1049V		Missense
Myelodysplastic (MSKCC, 2...	PD8533a	Acute Myeloid Leukemia	E646*		Nonsense
Myelodysplastic (MSKCC, 2...	PD9205a	Acute Myeloid Leukemia	X1310_splice		Splice
Myelodysplastic (MSKCC, 2...	PD9205a	Acute Myeloid Leukemia	W482*		Nonsense
Myelodysplastic (MSKCC, 2...	PD9282a	Acute Myeloid Leukemia	Q842*		Nonsense
Myelodysplastic (MSKCC, 2...	PD9300a	Acute Myeloid Leukemia	S1015N		Missense
Myelodysplastic (MSKCC, 2...	PD9306a	Acute Myeloid Leukemia	W591*		Nonsense
Myelodysplastic (MSKCC, 2...	PD9381a	Acute Myeloid Leukemia	A622V		Missense
Myelodysplastic (MSKCC, 2...	PD9381a	Acute Myeloid Leukemia	Q831*		Nonsense
Hypodiploid Acute Lymphoi...	SJHYPO042-D	B-Lymphoblastic Leukemia/Lymphoma	X809_splice Germline		Splice

Study of Origin	Sample ID	Cancer Type Detailed	Protein Change	Annotation	Mutation Type
Acute Myeloid Leuk...	aml_ohsu_20...	AML with Recurrent Geneti...	Y377C		Missense
Acute Myeloid Leuk...	aml_ohsu_20...	AML with Myelodysplasia-R...	C1509W		Missense
Acute Myeloid Leuk...	aml_ohsu_20...	AML with Myelodysplasia-R...	C1509W		Missense
Acute Myeloid Leuk...	aml_ohsu_20...	AML with Recurrent Geneti...	L861F		Missense
Myelodysplastic (M...	13-00622	AML with inv(3)(q21.3q26.2)...	Y377C		Missense
Myelodysplastic (M...	15-00056	AML with myelodysplasia-r...	C1509W		Missense
Myelodysplastic (M...	15-00057	AML with myelodysplasia-r...	C1509W		Missense
Myelodysplastic (M...	13-00654	Acute Myeloid Leukemia	L861F		Missense

Fig. S6. Mutational analyses of KDM5A and KDM5B in samples of AML and myeloid malignancy patients, based on cbioportal. (A) Overall rates of the indicated mutation of KDM5A/B in various myeloid malignancy cohorts. (B-C) Distribution of somatic mutation of KDM5B (B) and KDM5A (C) in the indicated AML or myeloid neoplasm patients.

Table S1. A list of 31 genes showing a common upregulation pattern among NUP98-NSD1- and MLL-AF9-transformed murine AML cells post-treatment of UNC1999, relative to DMSO, and in MLL-AF9+ AML cells post-depletion of Eed versus mock. The transcriptomic data of MLL-AF9+ murine AML cells were from our previously published paper: Supplemental Table S2 in [5]).

Agap1
Arhgap29
B93004
Cdc42bpa
Cdc42bpb
Cdkn2a
Dip2c
Dock7
Exoc6b
F14Rik
Fam46c
Frmd6
Galnt10
Gja1
Glcci1
Kdm5b
Lamc1
Lpl
Nqo1
Plxna1
Rxra
Serpine2
Slc6a8
Slc7a8
Spire1
Tgfbr3
Timp2
Tspan17
Vsig10
Zmat3
Zswim6

Table S2. List of differentially expressed genes (DEGs) showing significant up-regulation post- KD of Kdm5b, relative to mock, in NUP98-NSD1+ murine AML and showing significant down-regulation post-overexpression (OE) of Kdm5b, relative to mock, in MLL-AF9+ murine AML cells. DEGs are defined with a cutoff of adj p value of less than 0.05 and log2(fold-change) of over 0.20 for the genes with baseMean no less than 10. FC, fold change; q, adjusted p value. Red highlighted are genes related to AML stemness and/or aggressive growth.

Snhg17 Bnip3l Itgb7 Strbp Cenpn Rbm3 Gbp7 Tmem218 Sox4 Ttc39c Nol4l Tmsb10 Il1r1 Ankrd37 Gbe1 Dag1 Hmgb3 Lztfl1 Cd33 Tusc3 Mir17hg Sfr1 Arvcf Hnrnph1 Mdm1 Cytip Gm6166 Aldh18a1 Stxbp5 Tuba8 Fancl Rpl36a-ps2 Phf10 Nfix Vegfa 4930427A07Rik Slc7a5 Sh2d5 Ccnd1 Tnk2 Vamp8 Ube2g1 Tmem119 Prss57 Cux1 P4ha1 Anxa2 Pde4d Pold3 Mxd1 Snx30 Vezf1 Rell1 Tgfbr3l Lrrc42 Yars Cnn3 Fabp5 Pfkp Morf4l1 Id2 Fyttd1 C1galt1 Bace1 Pan2 Maff Pdk3 Tgtp2 Antxr2 Palm Gm5537 Pdcd10 Mob3a Mid1 Etv4 Kras Pcgf5 Khnyn Nsd1 Stk26 Btnl9 Rfx2 H2-T23 Fkbp5 Elk3 Ccne2 Kif22 Atp10a Txnip Tpi1 Ero1l Slc2a3 Gm10123 Clic4 Adgrg1 Jarid2 Myo1c Zcchc11 Ifi47 Spns3 Ggta1 Tax1bp1 Ccr1 Mgat5 Tsc22d3 Depdc1a H2-T24 Atf6 Fam160a2 D5Ertd605e Ubald2 Rgcc Oas2 Il12rb2 Muc13 Klhl23 Asap2 Pim1 Arl4a Hnrnph3 Fam63b Rora Acadm Nelfcd Lsm14b Samd9l Cd24a Bcr Uba7 Ift57 Snrpe Tagln2 Add3 Klf10 Mier3 Ptpn22 Ccnd2 Ssbp2 Hmgn5 Mndal Cebpe Flnb Cyb561a3 Otud7b F13a1 Mgat4b Thbs1 Fam133b Eno1 Aldoa Zfp395 Gm13456 Itih5 Pmaip1 Gm4617 Brd3 Tns1 Ramp1 P2ry14 Irf1 App Atp2b4 Cox20 Endod1 A430106G13Rik Trappc9 H1f0 Zc3hav1l Eif4ebp1 Ccnd3 Eno1b Stmn1 Mrpl23 Ptch1 Fam162a Kifap3 Ak4 Casp3 Gpnmb Lgals3 Cmpk2 Higd1a Smad7 Myb H3f3b Nipsnap1 Vps16 1700025G04Rik Treml2 Ksr1 Mxi1 Atf4 Fchsd2 Taf15 Dyrk3 Fcho1 Gadd45a Uimc1 Nos2 Ccnb2 Arhgap18 Vamp3 Lgals9 Pml Vbp1 Mcpt8 Bcl11a S100a8 Plgrkt Pgk1 Cds1 Cxcr2 Glipr2 Sell B4galt4 Prkca Gfod1 Rabgap1l Pdp1 Selp Lsm8 Cntnap1 Sema4b Hmga2 Slc1a4 H2afx Mgat4a Gng12 Nampt Fut7 Icam2 Gm11223 Tia1 Il18rap Elane Sp3 Ppp2r3c Hk1 Pan3 Cdc16 Mphosph6 Nsmaf Cenpk Plppr3 H2-Q7 Cd37 2510002D24Rik

Table S3. List of direct targets co-bound by Kdm5b and NUP98-NSD1, as well as showing significant up-regulation post-KD of Kdm5b, relative to mock, in murine AML cells. DEGs are defined with a cutoff of adj p value of less than 0.05 and log2(fold-change) of over 0.20 for the genes with baseMean no less than 10. FC, fold change; q, adjusted p value. **Red highlighted are genes related to AML stemness and/or aggressive growth.**

Katnbl1 Arhgap29 Nol4l Il10rb Nt5dc1 Fam117b Gnaq Zfp703 Gbe1 Stxbp5 Klf7 Runx2 Tuba8 Six1 Vegfa Ccnl2 Cux1 Vps39 Rabgap1 Rab22a Abtb1 Nphp3 Epm2a Stx6 Akip1 Esyt1 Hnrnpdl Arl8a Dennd3 Pdcd10 Slc32a1 Sh2b3 Znrf1 Plod1 Galnt11 Zc3h6 Ccne2 Stk25 Clic4 Myo1c Samd8 Atg10 Kif1b Fam69a Mtmr2 Tax1bp1 Crtc2 Fam160a2 Mfap3l Cyth1 Lsm14b Kdsr Lgalsl Inpp4a Ulk1 Add3 Map3k5 Fosl2 Gch1 Icosl Inip Ptbp2 Mthfd2l Irf1 Ankrd44 Cox20 Endod1 H1f0 Zc3hav1l Ccnd3 Btbd1 Raph1 Mrpl23 Thra Klhl17 Ddhd2 Med21 Ckap5 Tsc22d1 Kdelr1 Cep120 Kctd20 Snapin Uimc1 Mob1a Ifngr1 Hbp1 Naaa Dmxl2 Prkca Pdp1 Fbxl20 Me2 Sema4b Slc9a8 Mgat4a Gng12 Dtx3 Tia1 Leng8 Ifnar2 Cdkn2c Malt1 Laptm4a Nsmaf 8-Sep Hmg20b Fam117a Qsox2 Pink1 Ypel5 Zfand4 Tbcel Arhgap31 Slc7a5 Tex14 Ccnd1 Vamp8 Pcnx Mctp1 Btg1 Pygl Rnf38 Pold3 Vamp1 Gpt2 Adipor1 Fyn Tfdp2 Ncstn Asah1 Id2 Rsrc1 Sqstm1 Antxr2 Rab18 Fam168a Rcor3 Nr3c1 Hoxa7 Prdm4 Mob3a Kras Nsd1 Uba3 Tex2 Ero1l Rnf11 Paip2b Mgea5 Camkk2 Zswim6 Birc5 Mad2l1 Dleu2 Snrpe Pskh1 Prkch 6820431F20Rik Tmem65 Klf10 Rnf220 Irak1 Plxdc1 Atg16l1 Eno1 Csgalnact2 Dcaf6 Rcbtb2 G2e3 Ccdc69 Irs2 Ano10 Ankrd11 Pank2 Higd1a Smad7 Atf4 Rab5b Phf21a Hspa4l Lockd Fbxo25 Cdc42ep4 Auh 2-Mar Inpp5f Oxr1 Smc4 Emb Tmem181a Mnd1 Rnf19b Pan3 Foxo1 Ccsap Arrdc4 Cyb5r3 Sox4 Nfkbia Ankrd37 Sfr1 Mdm1 Cacna1b Phf10 Cebpg Rb1 Cdk1 Ube2g1 Trim3 Jak2 P4ha1 Rbpj Arsg Dcp1b Vezf1 Phactr4 Pde6d Kctd2 Nrbp1 Mettl23 Rfx2 Fbxl2 E2f6 Ifitm3 Dhrs3 Ptpn12 Msh5 Pias3 Slc44a1 Igf1r Mbtps1 Zfp523 Dcaf12 Hist1h1c Gpcpd1 Clk1 Fndc3b Clcn3 1810026B05Rik Ube2r2 Mapkapk3 Arl4a Spata6 Foxp1 Bcr Casp8 Cmtm3 Ttc17 Wdtc1 Tmbim6 Cebpe B4galt1 Trp53inp1 Klf2 Xpr1 Rsrp1 Otud7b Mgat4b Fam133b Tom1 Plcg1 Lrch1 Rcan3 Klhl5 Crk Hilpda Prkaca Ptch1 Rps23 Cwc15 Fchsd2 Atxn1l Papd4 Dgkg Tm7sf2 Osgin2 Gadd45a Vamp3 Btf3l4 Zfp810 Sft2d2 Cd164 Cds1 Gfod1 Adss Slc1a4 H2afx Nampt Gm16104 Yipf4 Fam45a Rab12 Unc13a E130307A14Rik Tmem229b Arvcf Hnrnph1 Parp8 Smim14 Adcy7 Sh2d5 Scarb2 Dync1li2 Iqsec2 Col5a3 Aplp2 Spag5 Calm2 Zc3h7a Fbxl5 Tm7sf3 Maff Acer3 Phf1 Mob2 Slc38a2 P2rx4 Ldlrad3 H2-T23 Fkbp5 Mbd6 Klf11 Tbc1d2b Pip5k1c Klf13 Jarid2 Zfr2 Furin Hp1bp3 Eef2k Pyroxd2 Pogk Kif23 Pim1 Sec22c Hnrnph3 Mtpn Egln1 Iffo1 Nt5c2 Epha7 Mier3 Tmx4 Cirbp Parp6 Ssbp2 Llgl1 Nfe2l1 Pten Orai1 Asb3 Rac1 Pmaip1 Maml1 Anln St6galnac6 Stmn1 Ddit4 Rufy2 Ksr1 Mxi1 Taf15 Dram1 Lrrfip2 Ccnb2 Atad1 Bcl11a Ube2z Rara Tagap1 Fam103a1 Sike1 Lsm8 Rbl1 Ebag9 Cebpa Inpp1 Cnot6l Ern1 Sp3 Mib2 Bmf

Supplementary References

1. Li, J., et al., *ZMYND11-MBTD1 induces leukemogenesis through hijacking NuA4/TIP60 acetyltransferase complex and a PWWP-mediated chromatin association mechanism.* Nat Commun, 2021. **12**(1): p. 1045.
2. Fan, H., et al., *BAHCC1 binds H3K27me3 via a conserved BAH module to mediate gene silencing and oncogenesis.* Nat Genet, 2020. **52**(12): p. 1384-1396.
3. Wang, G.G., et al., *NUP98-NSD1 links H3K36 methylation to Hox-A gene activation and leukaemogenesis.* Nat Cell Biol, 2007. **9**(7): p. 804-12.
4. Wang, G.G., et al., *Haematopoietic malignancies caused by dysregulation of a chromatin-binding PHD finger.* Nature, 2009. **459**(7248): p. 847-51.
5. Xu, B., et al., *Selective inhibition of EZH2 and EZH1 enzymatic activity by a small molecule suppresses MLL-rearranged leukemia.* Blood, 2015. **125**(2): p. 346-57.
6. Cai, L., et al., *ZFX Mediates Non-canonical Oncogenic Functions of the Androgen Receptor Splice Variant 7 in Castrate-Resistant Prostate Cancer.* Mol Cell, 2018. **72**(2): p. 341-354 e6.
7. Ren, Z., et al., *PHF19 promotes multiple myeloma tumorigenicity through PRC2 activation and broad H3K27me3 domain formation.* Blood, 2019. **134**(14): p. 1176-1189.
8. Konze, K.D., et al., *An orally bioavailable chemical probe of the Lysine Methyltransferases EZH2 and EZH1.* ACS chemical biology, 2013. **8**(6): p. 1324-34.
9. Souroullas, G.P., et al., *An oncogenic Ezh2 mutation induces tumors through global redistribution of histone 3 lysine 27 trimethylation.* Nat Med, 2016. **22**(6): p. 632-40.
10. Zhang, H., et al., *Oncogenic Deregulation of EZH2 as an Opportunity for Targeted Therapy in Lung Cancer.* Cancer Discov, 2016. **6**(9): p. 1006-21.
11. Lu, R., et al., *Epigenetic Perturbations by Arg882-Mutated DNMT3A Potentiate Aberrant Stem Cell Gene-Expression Program and Acute Leukemia Development.* Cancer Cell, 2016. **30**(1): p. 92-107.
12. Yu, X., et al., *A selective WDR5 degrader inhibits acute myeloid leukemia in patient-derived mouse models.* Sci Transl Med, 2021. **13**(613): p. eabj1578.
13. Dobin, A., et al., *STAR: ultrafast universal RNA-seq aligner.* Bioinformatics, 2013. **29**: p. 15-21.
14. Patro, R., et al., *Salmon provides fast and bias-aware quantification of transcript expression.* Nat Methods, 2017. **14**: p. 417-419.
15. Love, M.I., W. Huber, and S. Anders, *Moderated estimation of fold change and dispersion for RNA-seq data with DESeq2.* Genome Biol, 2014. **15**: p. 550.
16. Ahn, J.H., et al., *Phase separation drives aberrant chromatin looping and cancer development.* Nature, 2021. **595**(7868): p. 591-595.
17. Xu, C., et al., *Cistrome analysis of YY1 uncovers a regulatory axis of YY1:BRD2/4-PFKP during tumorigenesis of advanced prostate cancer.* Nucleic Acids Res, 2021. **49**(9): p. 4971-4988.
18. Fan, H., et al., *A conserved BAH module within mammalian BAHD1 connects H3K27me3 to Polycomb gene silencing.* Nucleic Acids Res, 2021. **49**(8): p. 4441-4455.